

Representation Learning with Fine-grained Patterns

Yuanhong Xu¹ Qi Qian^{1*} Hao Li¹ Rong Jin¹ Juhua Hu²

¹Alibaba Group

²School of Engineering and Technology University of Washington, Tacoma, USA

{yuanhong.xuyh, qi.qian, lihao.lh, jinrong.jr}@alibaba-inc.com, juhuah@uw.edu

Abstract

With the development of computational power and techniques for data collection, deep learning demonstrates a superior performance over most of existing algorithms on benchmark data sets. Many efforts have been devoted to studying the mechanism of deep learning. One important observation is that deep learning can learn the discriminative patterns from raw materials directly in a task-dependent manner. Therefore, the representations obtained by deep learning outperform hand-crafted features significantly. However, those patterns are often learned from super-class labels due to a limited availability of fine-grained labels, while fine-grained patterns are desired in many real-world applications such as visual search in online shopping. To mitigate the challenge, we propose an algorithm to learn the fine-grained patterns sufficiently when only super-class labels are available. The effectiveness of our method can be guaranteed with the theoretical analysis. Extensive experiments on real-world data sets demonstrate that the proposed method can significantly improve the performance on target tasks corresponding to fine-grained classes, when only super-class information is available for training.

1 Introduction

Deep learning attracts more and more attentions due to its tremendous success in computer vision [7, 9, 14] and NLP applications [5, 16]. With modern neural networks, deep learning can even achieve a better performance than human beings on certain fundamental tasks [9, 20]. The improvement from deep learning makes many applications, e.g., autonomous driving [2], visual search [19], question-answering system [25], etc. become feasible.

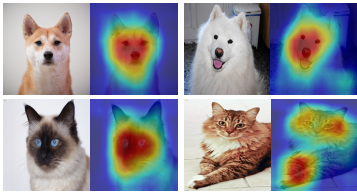


Figure 1: Illustration of spatial attention maps obtained by deep learning.

Evidently, the learned patterns can distinguish between “dogs” and “cats” well.

In deep learning, representations are often learned with the respect to specific tasks. Different patterns can be extracted even on the same data set for different application scenarios as shown in the example

Compared with most of existing models, which are designed for hand-crafted features, deep learning works in an end-to-end learning manner. It can explore the most discriminative patterns (i.e., features) from raw materials directly for the specific tasks. Without an explicit phase of generating features, deep learning demonstrates a significant improvement over existing methods [9, 14]. Using the features generated by deep learning, conventional methods can also perform better than the counterpart with hand-crafted features [1, 6, 7, 8]. This observation illustrates that neural networks can learn the task-related patterns sufficiently. Fig. 1 illustrates the spatial attention maps [26] discovered from a neural network.

*Corresponding author

of Fig. 2. The synthetic data contains 32 super-classes and 128 fine-grained classes. It can be observed that different discriminative patterns are obtained when the training task changes. The details about the experiment can be found in Section 4.1. This phenomenon demonstrates that neural networks will only pay attention to those patterns that are helpful for the training task and ignore the unrelated patterns. Therefore, deep learning has to access a massive amount of labeled examples to achieve the ideal performance while the label information has to be closely related to the target task.

With the development of deep learning, the importance of the scale of labeled data has been emphasized and many large-scale labeled data sets [4, 15] become available. However, the correlation between the learned representations using these labels and the target task is less investigated. In real-world applications, we are often more interested in the performance of the model on the task with fine-grained classes while the model can only be trained using labels from super-classes due to a limited availability of fine-grained labels. Taking visual search [19] as an example, for a query image of a husky, a result from the same species (i.e., huskies) is expected rather than a general one from the super-class of “dogs”. The problem becomes more challenging in the online shopping scenario, where many items (e.g., clothes) have very subtle differences. The gap between the available labels and the target task makes the learned representations suboptimal.

To improve the performance of models on the fine-grained classes, a straightforward way is to label a sufficient number of examples with fine-grained labels, which can align the supervised information and the target task well. However, this strategy is not affordable. Unlike super-class labels, fine-grained labels (e.g., species of dogs) can only be identified by very experienced experts, which is expensive and inefficient. For the visual search in the online shopping scenario, even experts cannot label massive examples accurately.

In this work, we aim to mitigate the issue by learning fine-grained patterns when only super-class labels are available. We find that fine-grained patterns, which are essential for distinguishing fine-grained classes, are often neglected when the deep model is trained with only super-class labels. Therefore, we propose to learn representations with fine-grained patterns by solving the basic super-class classification problem and a more challenging fine-grained categorization problem simultaneously. The main contribution of this work can be summarized as follows.

- We illustrate that the learned patterns in deep learning are closely related to the training task. The patterns can be different even on the same data with different labels (i.e., different application scenarios).
- We propose an algorithm to explore the fine-grained patterns sufficiently for the target task when the data in the training task and target task are from the same distribution but corresponding to labels of super-classes and fine-grained classes, respectively.
- We conduct extensive experiments on benchmark data sets to demonstrate that the proposed algorithm can improve the performance on real-world applications when only super-class labels are available.

2 Related Work

Different from many existing methods, CNNs can directly learn patterns from raw materials, which avoids the information loss in the phase of feature extraction. By investigating the patterns learned by CNNs, researchers find that it can adaptively figure out discriminative parts in images for classification due to the end-to-end learning manner [6, 14], which interprets the effectiveness of CNNs. However, the learned patterns are often closely related to the training task and CNNs can ignore the patterns that are not important for the current task. In terms of representation learning, when the target task is different from the training task in labels (e.g., only super-class labels are available for the training data while fine-grained labels are desired in the target task), the learned patterns can be suboptimal and thus not sufficient for the target task. In this work, we aim to learn representations with fine-grained patterns even when only super-class labels are available.

It should be noted that generalizing learned models for different target tasks has also been researched in transfer learning [22] and domain adaptation [24]. However, the problem addressed in this work is significantly different from them. Both of transfer learning and domain adaptation try to improve the performance on the target domain with the knowledge from a different source domain. In this work, we mitigate the performance degeneration on the fine-grained classes when learning representations from super-classes, which means the data are from the same domain but for different tasks. Besides,

our work is totally different from the research area of fine-grained visual categorization [3, 18] where fine-grained labels are available for training.

3 Learning Fine-grained Patterns

Given a set of images $\{(\mathbf{x}_i, y_i)\}_{i=1}^n$, a model can be learned by solving the optimization problem

$$\min_{\theta} \ell(\mathbf{x}_i, y_i; \theta)$$

where $\ell(\cdot)$ is the loss function and θ denotes the parameters of a neural network. Cross-entropy loss with the SoftMax operator is a popular loss in deep learning.

Many modern neural networks have multiple convolutional layers and a single fully-connected layer, e.g., ResNet [10], MobileNet [11], EfficientNet [23], etc. We will investigate this popular architecture in this work while the analysis can be extended to more generic structures.

For a C -class classification problem, the cross-entropy loss can be written as $\ell(\mathbf{x}_i, y_i) = -\log \frac{\exp(f(\mathbf{x}_i)^\top \mathbf{w}_{y_i})}{\sum_j^C \exp(f(\mathbf{x}_i)^\top \mathbf{w}_j)}$ where $f(\cdot)$ extracts features with convolutional layers from an image and $W = \{\mathbf{w}_1, \dots, \mathbf{w}_C\} \in \mathbb{R}^{d \times C}$ denotes the parameters of the last fully-connect layer in a neural network. d is the input dimensionality of the fully-connected layer.

Apparently, the behavior of function f heavily depends on the training labels of $\{y_i\}$. When the task implied by $\{y_i\}$ is consistent with the target one, the patterns discovered by f can perform well. However, when the training task is different from the target one (e.g., super-class training labels vs. fine-grained target task), the learned patterns can be suboptimal. In this work, we aim to learn an appropriate function f that can extract sufficient fine-grained patterns, even when only super-class labels are available.

In many real world applications, super-class labels (e.g., “dog”, “cat”, and “bird”) are easy to access. The problem with basic super-class labels can be defined as

$$\min_{\theta} \sum_i \ell(\mathbf{x}_i, y_i^B; \theta) \quad (1)$$

where $y_i^B \in \{1, \dots, B\}$ indicates the super-class of \mathbf{x}_i . The representations learned by this task can be inappropriate for the target task on fine-grained classes (e.g., “bulldog”, “husky”, and “poodle” under the super-class “dog”), which is

$$\min_{\theta} \sum_i \ell(\mathbf{x}_i, y_i^F; \theta) \quad (2)$$

where $y_i^F \in \{1, \dots, F\}$ indicates the fine-grained class of \mathbf{x}_i that is, however, not available for training. In this work, we assume that the fine-grained classes from different super-classes are not overlapped. The issue caused by the inconsistency in labels can be demonstrated as follows.

Proposition 1. *The patterns discovered by solving the problem with super-class labels in Eqn. 1 can fail to separate the examples with fine-grained class labels well.*

All detailed proof for this work can be found in the appendix. Here we give an example. Suppose we have three examples \mathbf{x}_1 , \mathbf{x}_2 and \mathbf{x}_3 . The corresponding labels can be $(y_1^B, y_2^B, y_3^B) = (\text{dog}, \text{dog}, \text{cat})$ and $(y_1^F, y_2^F, y_3^F) = (\text{husky}, \text{poodle}, \text{bengal})$. By optimizing the problem in Eqn. 1, we may obtain the features as

$$f(\mathbf{x}_1) = [1, 1, -1, -1]; \quad f(\mathbf{x}_2) = [1, 1, -1, -1]; \quad f(\mathbf{x}_3) = [-1, -1, 1, 1];$$

Those features can separate the examples on the super-classes well, while they cannot provide a meaningful separation for the fine-grained classes.

In fact, the patterns extracted for fine-grained classification can be totally different from those for identifying super-classes as illustrated in Fig. 2 (b). A straightforward way to address this discrepancy between the learned patterns and the target tasks is to solve the problem with fine-grained labels. However, fine-grained labels are often not affordable. With the observation that the patterns learned from Eqn. 1 lack the capability of distinguishing fine-grained classes, we propose a new optimization framework to increase the discrimination of learned representations.

Without extra supervised information, a problem that requests more discriminative patterns is to identify each individual example from the whole data set. The problem can be written as

$$\min_{\theta} \sum_i \ell(\mathbf{x}_i, y_i^I; \theta) \quad (3)$$

where $y_i^I \in \{1, \dots, n\}$ and $y_i^I = i$. The problem in Eqn. 3 considers that each example is from a different class and leads to a n -class classification problem. The problem is more challenging than the target one in Eqn. 2 and additional fine-grained patterns will be extracted to identify each example. However, the desired patterns for the target problem can be overwhelmed by too many patterns obtained from classifying individual examples. Therefore, the obtained patterns can still be far away from optimum as stated in the following proposition.

Proposition 2. *The patterns discovered by solving the problem of individual classification in Eqn. 3 cannot guarantee the performance on the fine-grained classification problem.*

Intuitively, many fine-grained patterns obtained from Eqn. 3 focus on distinguishing each individual example from others that may share the same fine-grained label, which will downgrade the performance on fine-grained classes.

Consequently, we consider to incorporate the problem in Eqn. 1 to guide the learning of fine-grained patterns in Eqn. 3. With the super-class label information, the model can explore the related fine-grained patterns more effectively. The problem can be written as

$$\min_{\theta} \sum_i \ell(\mathbf{x}_i, y_i^B) + \lambda_I \sum_i \ell(\mathbf{x}_i, y_i^I) \quad (4)$$

where λ_I is a trade-off between the super-class classification and individual classification. By optimizing the problem in Eqn. 4, we find that the performance of learned representations can be guaranteed on the fine-grained classes as follows.

Theorem 1. *By solving the problem in Eqn. 4, we assume that*

$$\forall i, \quad \Pr\{y_i^I | f(\mathbf{x}_i), W^I\} \geq \alpha; \quad \Pr\{y_i^B | f(\mathbf{x}_i), W^B\} \geq \beta$$

where α and β are constants that are balanced by λ_I . Besides, we assume $\forall i, j, \|f(\mathbf{x}_i)\|_2, \|\mathbf{w}_j\|_2 \leq c$ that their norms are bounded. Then, if each fine-grained class has z example, the performance of the learned representations $f(\mathbf{x})$ can be guaranteed on the target fine-grained problem as

$$\mathbb{E}[\Pr\{y_i^F | f(\mathbf{x}_i), W^F\}] \geq \alpha z h(c, \alpha, \beta)$$

where $h(c, \alpha, \beta) \leq 1$ is a constant that depends on c, α and β .

Concretely, with the help of Eqn. 1, we can bound the difference of examples from the same fine-grained class, while Eqn. 3 helps obtain sufficient fine-grained patterns for the target problem in Eqn. 2. When $\alpha > 1/n$ and β is optimized well, Theorem 1 shows that the prediction on the fine-grained problem can be better than $1/F$, where F is the number of fine-grained classes.

The subproblem of individual classification is comprised of a n -class classification problem. When n is large, it has to compute the scores and the corresponding gradient from $W^I \in \mathbb{R}^{d \times n}$ for each example, which can slow down the optimization significantly. In the following subsection, we discuss the strategy for speedup.

3.1 Large-scale Challenge

According to the analysis in Theorem 1, the patterns that separate examples from different super-classes can be captured by the super-class classification problem. Consequently, the individual classification can focus on distinguishing each individual example within the corresponding super-class. Therefore, we have the new objective as

$$\min_{\theta} \sum_i \ell(\mathbf{x}_i, y_i^B) + \lambda_I \sum_i \ell_B(\mathbf{x}_i, y_i^I) \quad (5)$$

where $\ell_B(\mathbf{x}_i, y_i^I) = -\log(\Pr\{y_i^I | \mathbf{x}_i, y_i^B, W^I\}) = -\log\left(\frac{\exp(f(\mathbf{x}_i)^\top \mathbf{w}_{y_i^I}^I)}{\sum_{j:j=y_i^B} \exp(f(\mathbf{x}_i)^\top \mathbf{w}_j^I)}\right)$.

Compared with the problem in Eqn. 4, the first subproblem remains the same while the second one is defined within each super-class in lieu of the whole data set. Therefore, the computational cost of the fully-connected layer for each example can be reduced from $\mathcal{O}(dn)$ to $\mathcal{O}(dn_b)$, where n_b denotes the number of examples in the b -th super-class.

We prove that the performance using the above speedup strategy can still be guaranteed on the target problem as stated in the following theorem.

Theorem 2. *With the similar assumptions as in Theorem 1 and*

$$\forall i, \quad \Pr\{y_i^I | \mathbf{x}_i, y_i^B, W^I\} \geq \alpha; \quad \Pr\{y_i^B | \mathbf{x}_i, W^B\} \geq \beta$$

by solving the problem in Eqn. 5, the performance of representations $f(\mathbf{x})$ can be guaranteed on the target problem as

$$\mathbb{E}[\Pr\{y_i^F | f(\mathbf{x}_i), W^F\}] \geq \alpha' z h(c, \alpha', \beta)$$

where $\alpha' = \frac{1}{1/\alpha + (1-\beta)c''/\beta}$. c'' is a constant and $h(c, \alpha', \beta)$ is a constant that depends on c , α' and β .

Remark Compared with the guarantee in Theorem 1, the cost of relaxation is given in α' . It contains a factor of $(1 - \beta)/\beta$, which measures the performance on the super-class classification problem. When an example can be separated well from other super-classes as $\beta \rightarrow 1$, the patterns obtained by solving Eqn. 5 can perfectly recover the results from solving the more expensive problem in Eqn. 4.

4 Experiments

We evaluate the proposed method on three real-world data sets. We adopt ResNet-18 [10] as the neural network for fair comparison since it is the most popular deep architecture and has been widely applied to real tasks. We include five methods in the comparison as follows.

- **Base**: optimize representations on super-classes only as in Eqn. 1.
- **Fine**: optimize representations on fine-grained classes with label information as in Eqn. 2.
- **Indi**: optimize representations on individual examples only as in Eqn. 3
- **Base-Indi**: learn representations with super-classes and individual classes as in Eqn. 4.
- **Base-Indi_{eff}**: improve the efficiency by optimizing the individual classes within each super-class as in Eqn. 5.

ResNet-18 is trained with stochastic gradient descent (SGD). All methods in the comparison have the same backbone network and training pipeline with different objectives. Augmentation is important for training CNNs and we adopt both random horizontal mirroring and random crop. Other configurations on each data set follow the common practice and are elaborated in the corresponding subsections.

We evaluate the performance of different models with multiple metrics. First, we measure the accuracy on super-classes. With more fine-grained patterns, the performance on super-classes may be further improved. Moreover, we evaluate the performance of representations on the fine-grained classes by conducting the retrieval task. It is a ubiquitous application scenario and we adopt Recall@ k metric as in [19, 21] for comparison.

4.1 Synthetic Data

Before evaluating the performance on real-world data sets, we conduct an experiment on the synthetic data to illustrate the difference between patterns learned using different levels of training labels on the same data set. The synthetic data is generated as shown in Fig. 2 (a). First, we randomly generate 32 big color patches and 128 small color patches as a pool of patches. Given a blank image, a big patch and a small patch are randomly sampled from the pool, and then added to the image. Finally, 512 images are obtained.

For the synthetic data, super-classes are defined with big patches and fine-grained classes are defined by small patches. Consequently, there are 32 super-classes and 128 fine-grained classes in the data set. To investigate the different patterns learned by the neural network, we train the model with the objective of Base, Fine and Indi, respectively. After that, we visualize the spatial attention maps

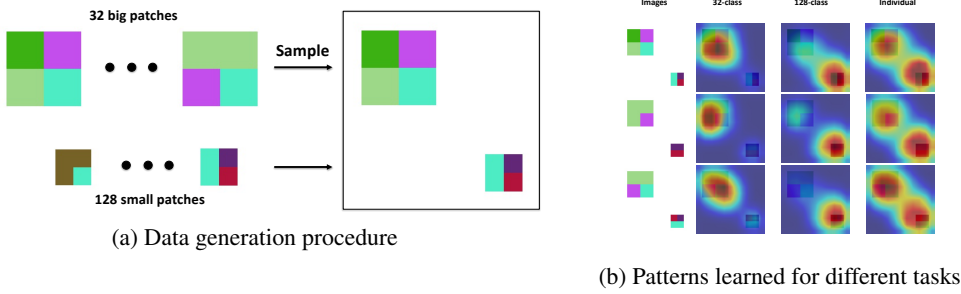


Figure 2: Synthetic Data.

with different models to illustrate the patterns exploited by these models. The detailed algorithm for computing attention maps can be found in [26].

Fig. 2 (b) shows the different attention maps. First, we can observe that deep learning can capture the most discriminative parts for a given task. For example, it can identify the big patches for 32-class classification task and the small patches for 128-class classification task. Second, the informative patterns for super-classes and fine-grained classes are totally different. When training the model with the objective in Eqn. 1 of Base, the neural network will ignore small patches, which are essential for the fine-grained class classification. Therefore, the patterns generated from the conventional pipeline can be inappropriate for the real-world applications as demonstrated in Proposition 1. Finally, optimizing the loss for identifying each example as Indi can explore all informative patterns in images sufficiently.

4.2 CIFAR-100

In this subsection, we evaluate the methods on CIFAR-100 [13] that contains 20 super-classes. Each super-class contains 5 fine-grained classes that contribute 100 fine-grained classes. We adopt the standard splitting, where each fine-grained class has 500 color images for training and 100 for test.

SGD with a mini-batch size of 256 is applied to learn the model. Following the common practice, we set momentum to 0.9 and weight decay as $5e^{-4}$. Each model is trained with 200 epochs. The initial learning rate is 0.1 and is decayed by a factor of 5 at $\{60, 120, 160\}$ epochs. The 32×32 images are randomly cropped from the zero-padded 40×40 images for the crop augmentation.

Table 1: Comparison of accuracy and recall (%) for 20 super-classes on CIFAR-100. (“-” means NA)

	Top1 Acc	Top5 Acc	R@1	R@2	R@4	R@8
Base	85.60	97.53	81.07	87.02	90.68	93.24
Indi	-	-	22.42	32.94	46.83	62.62
Base-Indi	86.27	98.15	82.38	87.97	91.42	94.10
Base-Indi _{eff}	86.08	97.92	82.28	87.51	91.43	94.15

Table 1 summarizes both the classification and retrieval performance on the 20 super-classes. First, it is surprising to observe that fine-grained patterns learned by Base-Indi can improve the performance on the original super-class classification problem. It illustrates that the task-dependent patterns learned by CNNs focus on the training task can be suboptimal for unseen examples of the same problem. Exploring more fine-grained patterns in training as suggested by Base-Indi can make the learned patterns generalize better on unseen data. Second, Base-Indi_{eff} has the similar performance as Base-Indi. It is consistent with the analysis in Theorem 2. The examples with super-class labels can be separated well on this data set with an accuracy more than 85%, which implies a large β in Theorem 2. Therefore, the performance of Base-Indi_{eff} can approach that of Base-Indi with significantly less computational cost. Note that there are 20 super-classes with the uniform distribution in this data set, the cost of computing the fully-connected layer for individual classification in Base-Indi_{eff} is only 5% of that in Base-Indi.

The similarity for retrieval is computed by the cosine similarity using the outputs before the fully-connected layer, i.e., $f(\mathbf{x})$. [19] shows that deep features learned by classification can capture the similarity between examples well.

A similar observation can be obtained for the retrieval task. First, all methods with the additional individual classification task can outperform the baseline with a significant margin. Besides, the algorithm with the improved efficiency performs similar to its original counterparts, which confirms the effectiveness of the proposed method. Finally, Indi is included in this comparison while it demonstrates the worst performance. It is because the task of individual classification cannot leverage the supervised information from the super-classes.

Table 2: Comparison of recall (%) for fine-grained classes on CIFAR-100 and Oxford-IIIT-Pet.

CIFAR-100					Oxford-IIIT-Pet				
	R@1	R@2	R@4	R@8		R@1	R@2	R@4	R@8
Base	37.06	51.63	67.04	79.91	Base	85.04	91.96	95.99	98.09
Indi	13.57	19.22	27.08	37.29	Base-Indi _{eff}	86.59	93.24	96.43	98.31
Base-Indi	56.95	67.97	77.50	85.50	Fine	92.23	95.83	97.41	98.56
Base-Indi _{eff}	56.62	68.04	77.46	85.11					
Fine	71.77	78.80	84.06	88.34					

Finally, the comparison on the retrieval task of 100 fine-grained classes is demonstrated in Table 2. Evidently, both Base and Indi cannot handle the retrieval task well on the fine-grained classes. As illustrated in our analysis, Base lacks the fine-grained patterns and Indi lacks the guidance to exploit the massive patterns for fine-grained classes. By combining their losses in Base-Indi, the performance can be dramatically improved. The R@1 of Base-Indi is better than Base by about 20% and surpasses Indi by more than 40%. It confirms the observation in Theorem 1 and shows that the proposed method can explore the fine-grained patterns sufficiently and effectively. Furthermore, Fine demonstrates the best performance when fine-grained labels are available for training. Compared to Fine, we can observe that R@4 of Base-Indi is better than R@1 of Fine and is comparable to R@2 of Fine. It means that when only labels for super-classes are available, by optimizing the objective in Eqn. 4, the learned model can handle the retrieval task well on fine-grained classes by retrieving two additional examples. Finally, the negligible difference between the performance of Base-Indi and Base-Indi_{eff} implies that the proposed algorithm is applicable for real-world applications.

4.3 Oxford-IIIT-Pet

Oxford-IIIT-Pet [17] data set consists of two super-classes: cats and dogs. There are 37 fine-grained classes, where 12 species are from cats and 25 species are from dogs. The total number of images is 7,349 and the provided splitting is applied for evaluation. Due to the limited number of training images, we initialize the parameters of the model with those pre-trained on ImageNet [4]. After that, each model is further fine-tuned on Oxford-IIIT-Pet by 30 epochs. The initial learning rate is 0.01 and decayed by a factor of 10 at the 15-th epoch.

Table 3: Comparison of accuracy and recall (%) for super-classes on Oxford-IIIT-Pet and SOP.

	Top1 Acc	Top5 Acc	R@1	R@2	R@4	R@8
Oxford-IIIT-Pet						
Base	99.62	100.00	99.73	99.84	99.92	99.97
Base-Indi _{eff}	99.67	100.00	99.86	99.89	99.97	100.00
SOP						
Base	80.12	97.30	76.56	84.29	89.50	93.21
Base-Indi _{eff}	80.56	97.45	77.08	84.54	89.71	93.40

As shown in Table 3, since the super-class labels are binary for the pet data, both of Base and Base-Indi_{eff} can achieve the ideal performance on this simple task. A similar phenomenon can be observed on the retrieval task.

Compared to the binary classification for super-classes, the task on fine-grained classes is more challenging. Table 2 summarizes the results on fine-grained classes. Despite the similar behaviors on super-classes, Base-Indi_{eff} demonstrates a margin of more than 1% over Base on R@1 for fine-grained classes. Note that the fine-grained classes in this data set are more similar than those in

CIFAR-100. The superior performance of Base-Indi_{eff} shows that the proposed method can explore patterns for subtle differences in images effectively. Besides, R@2 of Base-Indi_{eff} is better than R@1 of Fine. Therefore, our method can be helpful to recover the performance on fine-grained classes with an affordable cost from additional retrieved examples.

Fig. 3 (a) compares the retrieved images from different models. When training on super-classes, Base cannot identify the specified species in query images. For example, given an image of dog, Base can return an image similar to the query image as a dog but with a different fine-grained label. In contrast, Base-Indi_{eff} can learn details with the help from optimizing individual classification task and retrieve images from the same species successfully.

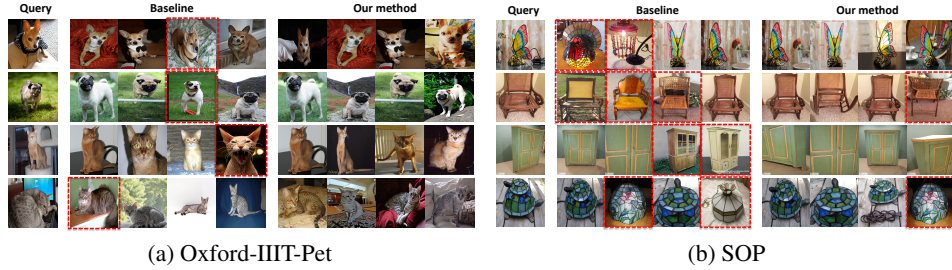


Figure 3: Examples of retrieved images from **Base** and **Base-Indi_{eff}**. The examples from a different fine-grained class are denoted with red bounding-boxes.

4.4 Stanford Online Products

Finally, we evaluate different algorithms in a challenging scenario of online shopping. Stanford Online Products (SOP) [21] collects 120,053 product images from eBay.com. There are a total of 22,634 fine-grained classes from 12 super-classes. Therefore, each fine-grained class contains very limited number of examples. Note that there is no public splitting on this data set for classification, so we randomly sample 80,000 images for training and the rest for test.

For training, we adopt the suggested configuration as in [10]. Specifically, the model is learned with 90 epochs. The initial learning rate is 0.1 and decayed by a factor of 10 at {30, 60} epochs. Results for super-class classification and retrieval are summarized in Table 3. It is evident that even when the target task is consistent with the training task, exploring fine-grained patterns can achieve additional gain.

The retrieval performance on the fine-grained classes is shown in Table 4. Considering the difficulty in this task, we report the Recall@{1,10,100,1000} in lieu of Recall@{1,2,4,8} as suggested in [19, 21]. First, we can observe that Base-Indi_{eff} outperforms Base by more than 10% on R@1. It demonstrates that our method can be applied for online shopping scenario when there is limited supervision. Besides, even with the supervised information on fine-grained classes, R@1 of Fine is less than 50%, which shows that retrieval in online shopping is an important but difficult application. With more retrieved examples, recall of Base-Indi_{eff} can approach 50% as shown in R@10. Note that customers for online shopping tend to review only the top ranked items, which is known as position bias [12]. Therefore, improving R@10 is important for better customer experience.

Table 4: Comparison of recall (%) for 22,634 fine-grained classes on SOP.

	R@1	R@10	R@100	R@1000
Base	20.77	33.82	52.37	78.34
Base-Indi _{eff}	32.56	47.99	65.39	82.95
Fine	45.93	61.52	75.42	87.96

We also illustrate the retrieved images on SOP in Fig. 3 (b). We can observe that there are many similar products from different fine-grained classes in online shopping, which makes the application very challenging. Given a query image, it is hard for Base to retrieve the appropriate items when training with the conventional pipeline. By learning fine-grained patterns sufficiently as in Base-Indi_{eff}, the similar examples with different labels are eliminated from the top ranked items.

5 Conclusion

Deep learning can extract representations from raw materials adaptively according to the training task. However, the conventional pipeline can be suboptimal since the learned models will focus on the training task and ignore massive fine-grained patterns in data, which can be potentially helpful for the task defined on fine-grained classes. In this work, we propose the algorithms to explore fine-grained patterns for real-world applications sufficiently. The empirical study on benchmark data sets confirms the effectiveness of our method. Considering that the number of unlabeled data is significantly larger than that of labeled data in real-world applications and the objective in Eqn. 3 is feasible for unlabeled data, incorporating unlabeled data to further improve the learning of fine-grained patterns can be our future work.

References

- [1] T. Chen, S. Kornblith, M. Norouzi, and G. E. Hinton. A simple framework for contrastive learning of visual representations. *CoRR*, abs/2002.05709, 2020.
- [2] X. Chen, H. Ma, J. Wan, B. Li, and T. Xia. Multi-view 3d object detection network for autonomous driving. In *CVPR*, pages 6526–6534, 2017.
- [3] Y. Cui, Y. Song, C. Sun, A. Howard, and S. J. Belongie. Large scale fine-grained categorization and domain-specific transfer learning. In *CVPR*, pages 4109–4118. IEEE Computer Society, 2018.
- [4] J. Deng, W. Dong, R. Socher, L. Li, K. Li, and F. Li. Imagenet: A large-scale hierarchical image database. In *CVPR*, pages 248–255, 2009.
- [5] J. Devlin, M. Chang, K. Lee, and K. Toutanova. BERT: pre-training of deep bidirectional transformers for language understanding. In *NAACL-HLT*, pages 4171–4186, 2019.
- [6] J. Donahue, Y. Jia, O. Vinyals, J. Hoffman, N. Zhang, E. Tzeng, and T. Darrell. Decaf: A deep convolutional activation feature for generic visual recognition. In *ICML*, pages 647–655, 2014.
- [7] R. B. Girshick, J. Donahue, T. Darrell, and J. Malik. Rich feature hierarchies for accurate object detection and semantic segmentation. In *CVPR*, pages 580–587, 2014.
- [8] K. He, H. Fan, Y. Wu, S. Xie, and R. B. Girshick. Momentum contrast for unsupervised visual representation learning. *CoRR*, abs/1911.05722, 2019.
- [9] K. He, G. Gkioxari, P. Dollár, and R. B. Girshick. Mask R-CNN. In *ICCV*, pages 2980–2988, 2017.
- [10] K. He, X. Zhang, S. Ren, and J. Sun. Deep residual learning for image recognition. In *CVPR*, pages 770–778, 2016.
- [11] A. G. Howard, M. Zhu, B. Chen, D. Kalenichenko, W. Wang, T. Weyand, M. Andreetto, and H. Adam. Mobilenets: Efficient convolutional neural networks for mobile vision applications. *CoRR*, abs/1704.04861, 2017.
- [12] T. Joachims, L. A. Granka, B. Pan, H. Hembrooke, and G. Gay. Accurately interpreting clickthrough data as implicit feedback. *SIGIR Forum*, 51(1):4–11, 2017.
- [13] A. Krizhevsky. Learning multiple layers of features from tiny images. 2009.
- [14] A. Krizhevsky, I. Sutskever, and G. E. Hinton. Imagenet classification with deep convolutional neural networks. In *NeurIPS*, pages 1106–1114, 2012.
- [15] T. Lin, M. Maire, S. J. Belongie, J. Hays, P. Perona, D. Ramanan, P. Dollár, and C. L. Zitnick. Microsoft COCO: common objects in context. In *ECCV*, pages 740–755, 2014.
- [16] T. Mikolov, I. Sutskever, K. Chen, G. S. Corrado, and J. Dean. Distributed representations of words and phrases and their compositionality. In *NeurIPS*, pages 3111–3119, 2013.
- [17] O. M. Parkhi, A. Vedaldi, A. Zisserman, and C. V. Jawahar. Cats and dogs. In *CVPR*, pages 3498–3505, 2012.
- [18] Q. Qian, R. Jin, S. Zhu, and Y. Lin. Fine-grained visual categorization via multi-stage metric learning. In *CVPR*, pages 3716–3724, 2015.
- [19] Q. Qian, L. Shang, B. Sun, J. Hu, H. Li, and R. Jin. Softtriple loss: Deep metric learning without triplet sampling. In *ICCV*, 2019.

- [20] F. Schroff, D. Kalenichenko, and J. Philbin. Facenet: A unified embedding for face recognition and clustering. In *CVPR*, pages 815–823, 2015.
- [21] H. O. Song, Y. Xiang, S. Jegelka, and S. Savarese. Deep metric learning via lifted structured feature embedding. In *CVPR*, pages 4004–4012, 2016.
- [22] C. Tan, F. Sun, T. Kong, W. Zhang, C. Yang, and C. Liu. A survey on deep transfer learning. In *ICANN*, pages 270–279, 2018.
- [23] M. Tan and Q. V. Le. Efficientnet: Rethinking model scaling for convolutional neural networks. In *ICML*, pages 6105–6114, 2019.
- [24] M. Wang and W. Deng. Deep visual domain adaptation: A survey. *Neurocomputing*, 312:135–153, 2018.
- [25] Z. Yang, X. He, J. Gao, L. Deng, and A. J. Smola. Stacked attention networks for image question answering. In *CVPR*, pages 21–29, 2016.
- [26] S. Zagoruyko and N. Komodakis. Paying more attention: Improving the performance of convolutional neural networks via attention transfer. In *ICLR*, 2017.

A Theoretical Analysis

A.1 Proof of Proposition 1

Proof. We show a counter example by assuming that the problem in Eqn. 1 can be solved such that

$$\forall i, j : y_i^B = y_j^B, \quad \|f(\mathbf{x}_i) - f(\mathbf{x}_j)\|_2 = 0$$

Then, for the problem with fine-grained labels, a good classifier should satisfy

$$\forall i, j : y_i^B = y_j^B, y_i^F \neq y_j^F, \quad \Pr\{y_i^F | \mathbf{x}_i, W^F\} \geq \Pr\{y_j^F | \mathbf{x}_i, W^F\}, \Pr\{y_j^F | \mathbf{x}_j, W^F\} \geq \Pr\{y_i^F | \mathbf{x}_j, W^F\}$$

Since $f(\mathbf{x}_i) = f(\mathbf{x}_j)$, we can replace \mathbf{x}_j with \mathbf{x}_i and have

$$\Pr\{y_j^F | \mathbf{x}_i, W^F\} \geq \Pr\{y_i^F | \mathbf{x}_i, W^F\}$$

Combining the inequalities, it obtains that

$$\Pr\{y_j^F | \mathbf{x}_i, W^F\} = \Pr\{y_i^F | \mathbf{x}_i, W^F\}$$

which shows that the classifier cannot identify fine-grained labels with representations learned by optimizing Eqn. 3. \square

A.2 Proof of Proposition 2

Proof. We take the XOR problem as a counter example. The problem is illustrated in Fig. 4. For individual classification as in Fig. 4 (a), each example can be linear separable with the learned representations. However, examples from the same fine-grained class cannot be linear separated in Fig. 4 (b).

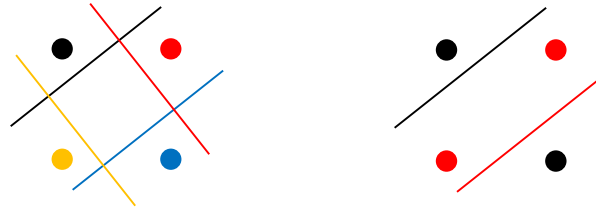


Figure 4: The counter example for representations learned from optimizing individual classification. Data points with the same color are from the same class. \square

A.3 Proof of Theorem 1

Proof. First, by optimizing the problem in Eqn 4, we assume

$$\forall i, \quad \Pr\{y_i^I | f(\mathbf{x}_i), W^I\} = \frac{\exp(f(\mathbf{x}_i)^\top \mathbf{w}_{y_i}^I)}{\sum_j^n \exp(f(\mathbf{x}_i)^\top \mathbf{w}_j^I)} \geq \alpha$$

and

$$\forall i, \quad \Pr\{y_i^B | f(\mathbf{x}_i), W^B\} = \frac{\exp(f(\mathbf{x}_i)^\top \mathbf{w}_{y_i}^B)}{\sum_j^B \exp(f(\mathbf{x}_i)^\top \mathbf{w}_j^B)} \geq \beta$$

By assuming the residual is lower bounded by constants a and b as

$$\forall i, \quad \sum_{j, j \neq y_i^I} \exp(f(\mathbf{x}_i)^\top \mathbf{w}_j^I) \geq a; \quad \sum_{j, j \neq y_i^B} \exp(f(\mathbf{x}_i)^\top \mathbf{w}_j^B) \geq b$$

we have

$$\exp(f(\mathbf{x}_i)^\top \mathbf{w}_{y_i}^I) \geq \frac{\alpha}{1-\alpha} \left(\sum_{j, j \neq y_i^I} \exp(f(\mathbf{x}_i)^\top \mathbf{w}_j^I) \right) \geq \frac{a\alpha}{1-\alpha}$$

and

$$\exp(f(\mathbf{x}_i)^\top \mathbf{w}_{y_i}^B) \geq \frac{\beta}{1-\beta} \left(\sum_{j, j \neq y_i^B} \exp(f(\mathbf{x}_i)^\top \mathbf{w}_j^B) \right) \geq \frac{b\beta}{1-\beta}$$

which leads to

$$\forall i, \quad f(\mathbf{x}_i)^\top \mathbf{w}_{y_i}^I \geq \log\left(\frac{a\alpha}{1-\alpha}\right); \quad f(\mathbf{x}_i)^\top \mathbf{w}_{y_i}^B \geq \log\left(\frac{b\beta}{1-\beta}\right)$$

To simplify the proof, we assume that each fine-grained class contains z examples as $zF = n$. Since W^F optimizes the target problem, we have

$$\mathbb{E}[\Pr\{y_i^F | f(\mathbf{x}_i), W^F\}] = \mathbb{E}\left[\frac{\exp(f(\mathbf{x}_i)^\top \mathbf{w}_{y_i}^F)}{\sum_j^F \exp(f(\mathbf{x}_i)^\top \mathbf{w}_j^F)}\right] \geq \mathbb{E}\left[\frac{\exp(f(\mathbf{x}_i)^\top \bar{\mathbf{w}}_{y_i}^I)}{\sum_s^F \exp(f(\mathbf{x}_i)^\top \bar{\mathbf{w}}_s^I)}\right]$$

where $\bar{\mathbf{w}}_s^I = \frac{1}{z} \sum_{y_j^F=s} \mathbf{w}_j^I$ averaging over the parameters from the same fine-grained class. According to the Jensen's inequality, we have

$$\exp(f(\mathbf{x}_i)^\top \bar{\mathbf{w}}_s^I) \leq \frac{1}{z} \sum_{y_j^F=s} \exp(f(\mathbf{x}_i)^\top \mathbf{w}_j^I)$$

Therefore, we have

$$\begin{aligned} \mathbb{E}[\Pr\{y_i^F | f(\mathbf{x}_i), W^F\}] &\geq \mathbb{E}\left[\frac{\exp(f(\mathbf{x}_i)^\top \bar{\mathbf{w}}_{y_i}^I)}{\frac{1}{z} \sum_j^n \exp(f(\mathbf{x}_i)^\top \mathbf{w}_j^I)}\right] \\ &\geq \mathbb{E}[z \exp(f(\mathbf{x}_i)^\top \bar{\mathbf{w}}_{y_i}^I) - f(\mathbf{x}_i)^\top \mathbf{w}_{y_i}^I] \Pr\{y_i^I | \mathbf{x}_i, W^I\} \\ &\geq z\alpha \mathbb{E}[\exp(f(\mathbf{x}_i)^\top \bar{\mathbf{w}}_{y_i}^I) - f(\mathbf{x}_i)^\top \mathbf{w}_{y_i}^I] \end{aligned} \quad (6)$$

where $\mathbb{E}[\exp(f(\mathbf{x}_i)^\top \bar{\mathbf{w}}_{y_i}^I) - f(\mathbf{x}_i)^\top \mathbf{w}_{y_i}^I]$ measures the distance from individual example to other examples from the same fine-grained class. It cannot be bounded well by only solving the problem in Eqn. 3.

To guarantee the performance on the fine-grained classification, we have to bound $\mathbb{E}[\exp(f(\mathbf{x}_i)^\top \bar{\mathbf{w}}_{y_i}^I) - f(\mathbf{x}_i)^\top \mathbf{w}_{y_i}^I]$ as illustrated in Eqn. 6. Now, it can be bounded with the help from solving the super-class classification.

$$\begin{aligned} &f(\mathbf{x}_i)^\top \mathbf{w}_j^I - f(\mathbf{x}_i)^\top \mathbf{w}_{y_i}^I \\ &= f(\mathbf{x}_i)^\top f(\mathbf{x}_j) + f(\mathbf{x}_i)^\top (\mathbf{w}_j^I - f(\mathbf{x}_j)) - f(\mathbf{x}_i)^\top f(\mathbf{x}_i) + f(\mathbf{x}_i)^\top (f(\mathbf{x}_i)^\top - \mathbf{w}_{y_i}^I) \end{aligned}$$

We can bound each terms as follows.

First, the distance of the examples to its individual label can be bounded by solving the individual classification problem.

$$\begin{aligned}
f(\mathbf{x}_i)^\top (\mathbf{w}_j^I - f(\mathbf{x}_j)) &\geq -\|f(\mathbf{x}_i)^\top (\mathbf{w}_j^I - f(\mathbf{x}_j))\|_2 \\
&\geq -\|f(\mathbf{x}_i)\|_2 \|\mathbf{w}_j^I - f(\mathbf{x}_j)\|_2 \text{(Cauchy-Schwarz inequality)} \\
&\geq -c \|\mathbf{w}_j^I - f(\mathbf{x}_j)\|_2 \\
&\geq -c \sqrt{2c^2 - 2 \log(a\alpha/(1-\alpha))}
\end{aligned}$$

With the similar analysis, we have

$$f(\mathbf{x}_i)^\top (f(\mathbf{x}_i)^\top - \mathbf{w}_{y_i}^I) \geq -c \sqrt{2c^2 - 2 \log(a\alpha/(1-\alpha))}$$

Note that examples from the same fine-grained class also share the same label of super-classes. Therefore, the distances between examples from the same fine-grained class can be bounded as

$$\begin{aligned}
f(\mathbf{x}_i)^\top f(\mathbf{x}_j) - f(\mathbf{x}_i)^\top f(\mathbf{x}_i) &\geq -c \|f(\mathbf{x}_j) - f(\mathbf{x}_i)\|_2 \\
&\geq -c (\|f(\mathbf{x}_j) - \mathbf{w}_{y_i}^B\|_2 + \|f(\mathbf{x}_i) - \mathbf{w}_{y_i}^B\|_2) \\
&\geq -2c \sqrt{2c^2 - 2 \log(b\beta/(1-\beta))}
\end{aligned}$$

Combine them together, we have

$$\begin{aligned}
&\exp(f(\mathbf{x}_i)^\top \bar{\mathbf{w}}_{y_i}^I - f(\mathbf{x}_i)^\top \mathbf{w}_{y_i}^I) \\
&\geq \exp\left(-\frac{2c(z-1)}{z}(\sqrt{2c^2 - 2 \log(a\alpha/(1-\alpha))} + \sqrt{2c^2 - 2 \log(b\beta/(1-\beta))})\right)
\end{aligned}$$

Taking it back to Eqn. 6, we can observe the desired result

$$\mathbb{E}[\Pr\{y_i^F | f(\mathbf{x}_i), W^F\}] \geq \alpha z h(c, \alpha, \beta)$$

where

$$h(c, \alpha, \beta) = \exp\left(-\frac{2c(z-1)}{z}(\sqrt{2c^2 - 2 \log(a\alpha/(1-\alpha))} + \sqrt{2c^2 - 2 \log(b\beta/(1-\beta))})\right)$$

□

A.4 Proof of Theorem 2

Proof. Following the analysis in Theorem 1, we assume

$$\begin{aligned}
\forall i, \quad \Pr\{y_i^I | \mathbf{x}_i, y_i^B, W^I\} &= \frac{\exp(f(\mathbf{x}_i)^\top \mathbf{w}_{y_i}^I)}{\sum_{j:j=y_i^B} \exp(f(\mathbf{x}_i)^\top \mathbf{w}_j^I)} \geq \alpha \\
\forall i, \quad \Pr\{y_i^B | \mathbf{x}_i, W^B\} &= \frac{\exp(f(\mathbf{x}_i)^\top \mathbf{w}_{y_i}^B)}{\sum_j \exp(f(\mathbf{x}_i)^\top \mathbf{w}_j^B)} \geq \beta \\
\forall i, \quad \sum_{j=y_i^B, j \neq y_i^I} \exp(f(\mathbf{x}_i)^\top \mathbf{w}_j^I) &\geq a; \quad \sum_{j \neq y_i^B} \exp(f(\mathbf{x}_i)^\top \mathbf{w}_j^B) \geq b
\end{aligned}$$

Compared with the analysis for Theorem 1, if we can bound $\Pr\{y_i^I | \mathbf{x}_i, W^I\}$, the performance on the fine-grained classification can be guaranteed. First, we try to bound the similarity between the example and the individual classes. Considering $\forall j, j \neq y_i^B$, we have

$$\begin{aligned}
f(\mathbf{x}_i)^\top \mathbf{w}_j^I &= f(\mathbf{x}_i)^\top f(\mathbf{x}_j) + f(\mathbf{x}_i)^\top (\mathbf{w}_j^I - f(\mathbf{x}_j)) \\
&\leq f(\mathbf{x}_i)^\top f(\mathbf{x}_j) + c \|\mathbf{w}_j^I - f(\mathbf{x}_j)\|_2 \\
&\leq f(\mathbf{x}_i)^\top \mathbf{w}_j^B + c(\|f(\mathbf{x}_j) - \mathbf{w}_j^B\|_2 + \|\mathbf{w}_j^I - f(\mathbf{x}_j)\|_2)
\end{aligned}$$

Note that

$$(1 - \beta) \exp(f(\mathbf{x}_i)^\top \mathbf{w}_{y_i}^B) \geq \beta \sum_{j \neq y_i^B}^B \exp(f(\mathbf{x}_i)^\top \mathbf{w}_j^B)$$

we have

$$\forall j \neq y_i^B, \quad f(\mathbf{x}_i)^\top \mathbf{w}_j^B \leq \log\left(\frac{1 - \beta}{\beta}\right) + f(\mathbf{x}_i)^\top \mathbf{w}_{y_i}^B$$

Therefore, the similarity can be further bounded as

$$\begin{aligned} f(\mathbf{x}_i)^\top \mathbf{w}_j^I &\leq \log\left(\frac{1 - \beta}{\beta}\right) + f(\mathbf{x}_i)^\top \mathbf{w}_{y_i}^B + c(\|f(\mathbf{x}_j) - \mathbf{w}_j^B\|_2 + \|\mathbf{w}_j^I - f(\mathbf{x}_j)\|_2) \\ &\leq \log\left(\frac{1 - \beta}{\beta}\right) + f(\mathbf{x}_i)^\top (\mathbf{w}_{y_i}^B - \mathbf{w}_j^I + \mathbf{w}_j^I) + c(\|f(\mathbf{x}_j) - \mathbf{w}_j^B\|_2 + \|\mathbf{w}_j^I - f(\mathbf{x}_j)\|_2) \\ &\leq \log\left(\frac{1 - \beta}{\beta}\right) + f(\mathbf{x}_i)^\top \mathbf{w}_{y_i}^I + c(\|\mathbf{w}_{y_i}^B - \mathbf{x}_i\|_2 + \|\mathbf{x}_i - \mathbf{w}_{y_i}^I\|_2 + \|f(\mathbf{x}_j) - \mathbf{w}_j^B\|_2 + \|\mathbf{w}_j^I - f(\mathbf{x}_j)\|_2) \end{aligned}$$

Note that the distance between the example and its corresponding parameters \mathbf{w}_i can be bounded as in Theorem 1, we have

$$\forall i, j : j \neq y_i^B, \exp(f(\mathbf{x}_i)^\top \mathbf{w}_j^I) \leq \frac{1 - \beta}{\beta} c' \exp(f(\mathbf{x}_i)^\top \mathbf{w}_{y_i}^I)$$

where

$$c' = \exp(2c(\sqrt{2c^2 - 2\log(a\alpha/(1 - \alpha))} + \sqrt{2c^2 - 2\log(b\beta/(1 - \beta))}))$$

Then, we have

$$\begin{aligned} \Pr\{y_i^I | \mathbf{x}_i, W^I\} &= \frac{\exp(f(\mathbf{x}_i)^\top \mathbf{w}_{y_i}^I)}{\sum_j^n \exp(f(\mathbf{x}_i)^\top \mathbf{w}_j^I)} \\ &= \frac{1}{\frac{\sum_{j:j=y_i^B} \exp(f(\mathbf{x}_i)^\top \mathbf{w}_j^I)}{\exp(f(\mathbf{x}_i)^\top \mathbf{w}_{y_i}^I)} + \frac{\sum_{j:j \neq y_i^B} \exp(f(\mathbf{x}_i)^\top \mathbf{w}_j^I)}{\exp(f(\mathbf{x}_i)^\top \mathbf{w}_{y_i}^I)}} \\ &\geq \frac{1}{1/\alpha + (1 - \beta)c'M/\beta} \end{aligned}$$

where M denotes the quantity of examples from different super-classes as $M = |\{\mathbf{x}_j : y_j^B \neq y_i^B\}|$. Let

$$\alpha' = \frac{1}{1/\alpha + (1 - \beta)c''/\beta}$$

where $c'' = c'M$, and we can obtain the guarantee by the similar analysis as in Theorem 1. \square